Cleaner Engineering and Technology 33 (2026) 101266

Contents lists available at ScienceDirect

Cleaner Engineering and Technology

journal homepage: www.sciencedirect.com/journal/cleaner-engineering-and-technology

Repairable photovoltaic modules: Repairability assessment and reliability-based design optimization under uncertain loading

A.G. Timmers Verhoeven [a], Z. Fung-A-Jou [b], S. Brinksma [b], O. Nejadseyfi [a,*]

[a] Computational Design and Mechanics, Precision and Microsystems Engineering Department, Faculty of Mechanical Engineering, Delft University of Technology, Delft, The Netherlands

[b] Research and development department, Biosphere Solar B.V., Rotterdam, The Netherlands

ARTICLE INFO

Dataset link: https://github.com/atimmersverhoe/RobustimizerSolar

Keywords:
Repairability assessment
Reliability-based optimization
Sustainable manufacturing
Design for repair
Solar panel
Right to repair

ABSTRACT

As the solar industry continues to grow, the accumulation of photovoltaic (PV) module waste highlights the pressing need for more circular, modular and repairable designs. Conventional laminated modules are difficult to disassemble, which limits not only their repairability but also material recovery and component reuse during recycling. While avoiding the lamination improves disassembly, it also compromises the module's mechanical integrity. This trade-off demands a careful redesign to maintain structural requirements without sacrificing key criteria such as repairability, weight, and cost. Existing repairability assessment methods are generally not tailored to PV modules and are rarely integrated with reliability-based design optimization to balance repairability, structural performance, weight, and cost during the early design phase. This study presents a semi-quantitative relative repairability assessment method, tailored specifically for PV modules, to quantify the impact of design changes on repairability. Additionally, a reliability-based optimization approach is presented to redesign the PV module. Using Robustimizer software, reliability-based optimization is incorporated to account for uncertain scenarios during the life cycle of the product. As a case study, the proposed methodologies are applied to a laminate-free open-source PV module developed by Biosphere Solar. Finite element analysis and experimental testing on a prototype demonstrate compliance with IEC61215 standard. The optimized design achieved a 51% improvement in repairability compared to the baseline design, together with a 6% reduction in cost, albeit at the expense of a 45% increase in module mass. The proposed approach provides a scalable framework for advancing sustainable design practices in the PV industry.

1. Introduction

The solar industry plays a crucial role in the transition toward a circular economy, offering renewable energy solutions that reduce dependence on fossil fuels and lower carbon emissions. Many studies focus primarily on improving operational efficiency, for example through active cooling systems that enhance thermal performance (Srithar et al., 2025) or advanced neural network models for orientation optimization and prediction accuracy (AL-Rousan and AL-Najjar, 2024). However, limited attention has been given to the circularity and repairability of PV module design. Traditional PV modules consist of several key layers and components working together to ensure efficiency and durability. The solar cells are encapsulated between two layers of Ethylene Vinyl Acetate (EVA), which enhance the durability and performance of solar modules. These layers hold the cells securely between the glass and the backsheet, absorb shocks and vibrations, and shield the fragile cells and their circuits from damage. Similar encapsulation concepts are also employed in bifacial PV modules which allow light collection from both sides of the solar cells.

While the use of the EVA layer in PV modules initially appears to offer substantial advantages, a major drawback of the laminated design is that it is incredibly challenging to recycle or repair, often requiring energy-intensive processes that are neither cost-effective nor effective at material recovery (Chowdhury et al., 2020; Ndalloka et al., 2024). The use of harmful substances, solvents, or energy-intensive conditions during recycling (Khetri and Gupta, 2025; T. Chowdhury et al., 2026), the difficulty of opening and separating the layered structure (Karagöz et al., 2025), and concerns regarding economic viability (Padhamnath et al., 2025) remain significant barriers to the sustainable end-of-life management of PV modules. This results in a significant waste problem as damaged or end-of-life panels are often discarded rather than refurbished or repurposed. This issue is particularly concerning given that the solar industry is rapidly expanding both in Europe and

* Corresponding author.
E-mail address: o.nejadseyfi@tudelft.nl (O. Nejadseyfi).

https://doi.org/10.1016/j.clet.2026.101266
Received 23 February 2026; Received in revised form 23 June 2026; Accepted 24 June 2026
Available online 24 July 2026

globally. Globally, it is estimated that approximately 75 TW of installed PV capacity will be required by 2050 (Haegel et al., 2023). By 2050, the European Union is expected to generate between 21 and 35 million tonnes of solar panel waste, while globally, the accumulation could reach up to 160 million tons (Foster et al., 2025). To put this into perspective, global electronic waste generation was estimated at 62 million tonnes in 2022 alone (Baldé et al., 2024). Although PV waste is accumulated over several decades, these projections highlight the scale of the emerging end-of-life challenge associated with photovoltaic technologies. This waste includes valuable materials such as aluminum, copper, silver, tin, glass, and silicon (Weckend et al.; P. Chowdhury et al., 2026).

Several early attempts have been made to recover PV module materials after disposal (Yao et al., 2025). For instance, Wambach (2009) demonstrated the technical feasibility of recovering and purifying silicon from end-of-life c-Si PV panels. Their method involved pyrolysis to remove metallization and dopant layers, followed by selective etching to produce a new silicon ingot (Wambach, 2009). A similar process was developed by the Japanese NEDO program through the Foundation for Advancement of International Science (FAIS), which also relies on pyrolysis of the polymers in a conveyor kiln (Weckend et al.).

More recently, alternative recycling strategies have been developed to improve material recovery while reducing environmental impact. For example, enzymatic delamination methods have been proposed for the separation of EVA layers, offering a potentially less aggressive alternative to conventional thermal and chemical treatments (Karagöz et al., 2025). Other studies have investigated solvent-assisted and advanced separation approaches to improve EVA removal and material recovery efficiency, although challenges related to solvent consumption, process complexity, and secondary waste generation remain significant Khetri and Gupta (2025), T. Chowdhury et al. (2026). Furthermore, recent life-cycle assessments indicate that while improved recycling routes and direct reuse of recovered PV glass can reduce environmental impacts, the recovery processes themselves may still contribute significantly to energy consumption and emissions (T. Chowdhury et al., 2026).

Despite these technological advances, separating materials from the EVA encapsulant remains a challenging, energy-intensive, and costly process, often resulting in contaminated recovered materials (Sivagami et al., 2024). In addition, achieving economically viable, scalable, and high-purity recovery of PV module materials remains a major challenge for the widespread implementation of circular PV systems (Späth et al.; Padhamnath et al., 2025). Addressing these limitations is thus essential for enhancing the sustainability and circularity of solar technologies, ensuring that the industry not only produces clean energy but also minimizes its own environmental footprint throughout the product's lifecycle.

In parallel with advances in recycling technologies, increasing attention is being given to the concept of the "right to repair", which seeks to extend product lifetimes by facilitating maintenance, repair, and component replacement. Recent policy initiatives, particularly within the European Union, encourage product designs that improve repairability and reduce premature disposal. While such efforts have gained significant traction in consumer electronics and household appliances, their application to photovoltaic modules remains limited due to the highly integrated and laminated nature of conventional PV designs. Consequently, incorporating repairability considerations during the design stage represents a promising pathway toward more circular and resource-efficient photovoltaic systems.

There are several strategies to increase the circularity of a product, which is summarized in Fig. 1: Refuse, Rethink, Reduce, Reuse, Repair, Refurbish, Remanufacture, Repurpose, and Recycle (Kirchherr and Piscicelli, 2019). Integrating these strategies enables a transition from a linear to a circular economy, maximizing product lifecycle and minimizing waste, with Refuse (R0) being the most favorable and Recover (R9) the least. Since the solar industry provides a far better solution compared to other energy alternatives, it should not be refused or reduced. Instead, the focus should shift toward enhancing reuse and repair rather than solely relying on recycling or material recovery. Research on PV module designs focused on improved repairability or reusability is hardly addressed and only a few studies can be found in literature. One such technology is the NICE technology (Dupuis et al., 2012), in which, contrary to standard modules, they use under-pressure within the module, causing the front and back glass layers to press copper ribbons directly onto the cell busbars. As a result, this approach eliminates the need for soldering and EVA-like encapsulants. Another approach is the modular PV module proposed by Majdi et al. (2021) in which they proposed building PV modules from many small, self-contained cell units, thereby improving repairability, reducing lifecycle costs, and lowering e-waste. From both repairing and recycling perspectives, these designs enable the recovery of entire components such as glass, copper tabs, and solar cells at low-cost and with negligible amount of contamination by other materials, resulting in clean residue-free surfaces (Einhaus et al., 2018). A similar yet distinct route is adopted in open-source hardware design by Biosphere Solar which is creating a modular, circular, and transparent PV module using sustainable production techniques to promote clean energy accessibility. To avoid lamination, this design uses a polyisobutylene (PIB) seal around the edge of the module together with small internal PIB dots placed between the solar cells to keep them in place, connect them to the glass plates, and provide mechanical rigidity as shown in Fig. 2.

To access and repair or recycle internal components such as the solar cells, the frame is first removed. Next, the edge seal and adhesive dots are cut using a hot knife or wire cutter, allowing the glass layers to be separated and the internal components to be reached. Without the lamination process, this design allows for the reuse, repair, and recycling of major components while minimal energy is required for disassembly, as the process involves mechanical separation rather than for instance high-temperature methods. Due to the absence of the EVA layer, one major drawback of such designs is the limited mechanical strength which creates challenges in meeting the requirements as specified in the IEC61215 standard for PV modules (International Electrotechnical Commission, 2021). Since there are many design choices to improve mechanical strength, trial-and-error is not only costly but infeasible to explore the design space efficiently. At the same time, those design choices should not come at the expense of key factors such as weight, cost, and repairability. Initial prototypes using this open-source design led to early failure due to limited mechanical strength. This highlights the need for a systematic, combined optimization approach that simultaneously considers structural performance, repairability, cost, and mass to arrive at a viable, balanced design. This challenge is complicated by the absence of a standardized method to evaluate or compare the repairability of solar panel designs. Yet, to effectively design or redesign for repairability, it is crucial to establish a clear and consistent framework for how repairability is assessed. Another complication is the fact that both modeling and real-world applications involve inherent uncertainty. A common engineering response is to apply conservative safety margins to account for these unknowns. However, while this approach increases robustness, it can also result in unnecessary overdesign, adding weight or cost that may not be needed or lead to inefficient material use.

These challenges have not yet been addressed systematically in the literature. Therefore, this study addresses two primary research gaps:

The development of a methodology to evaluate and quantify the repairability of solar modules and to integrate this metric into an optimization framework.

The implementation of a reliability based optimization algorithm to systematically account for uncertainties in the design process of PV modules, thereby reducing the reliance on conservative safety margins and minimizing the need for costly trial-and-error approaches.

As a case study, the developed methodologies are applied to the open-source Biosphere solar PV module design to demonstrate their

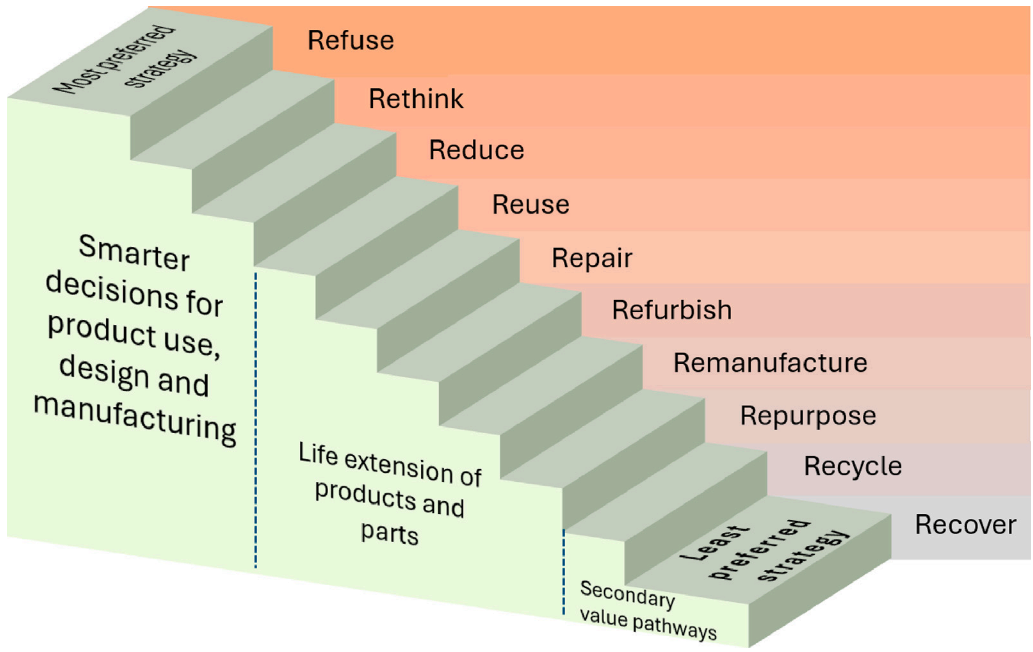

Fig. 1. Hierarchy of circular economy strategies, ordered from most preferred (Top) to least preferred (Bottom)

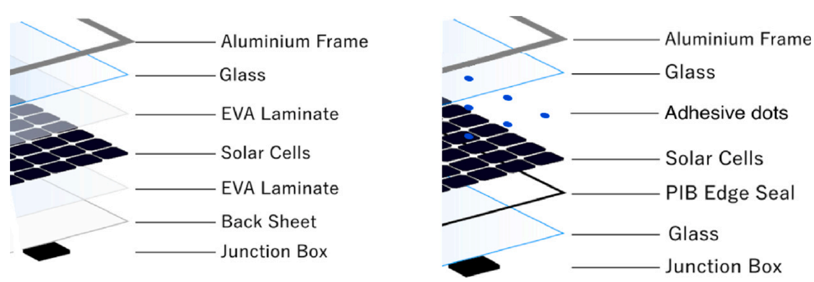

Fig. 2. Traditional (Laminated) PV module stack *(left)* and glass–glass laminate-free Biosphere PV module V1.3 *(right)*.

relevance and applicability. More broadly, the proposed approach offers a scalable framework for all solar technology developers in making informed design decisions during early-stage product development.

Section 2, introduces general repairability assessment methods and proposes a tailored assessment method for evaluating the repairability of PV module designs. Additionally, it covers the finite element modeling, optimization approach and reliability based techniques. Section 3 describes the validation of the finite element model through experimental testing and presents results and discussions. Section 4 is allocated for discussing the limitations and recommendations for future directions.

2. Methods

2.1. Assessing repairability

2.1.1. Repairability assessment methods

To effectively improve a product's repairability during (re)design, it is essential to have a clear and precise definition of how repairability is assessed. During the last few years, in line with the European Regulatory Framework, several initiatives have been introduced with the aim of assessing the level of repairability of different products (Blanco-Espeleta et al., 2024). The methods described in the literature can be divided into three categories:

- Qualitative methods that establish pass-fail criteria
- Semi-quantitative methods that allow to compare products within a specific family
- Quantitative methods that use measurable data to evaluate aspects such as the ease of disassembly.

One qualitative method is the method developed by Cordella et al. (2018) where a product-specific checklist of variables and conditions was developed that positively influence the repairability and upgradability of Energy related Products (ErP) (Cordella et al., 2018). Within semi-quantitative approaches, the Assessment Matrix for ease of Repair (AsMeR) (Bracquené et al., 2018) and the Repair Scoring System (RSS) (Spiliotopoulos et al.) are the most commonly used (Rodríguez and Favi, 2022). These methods calculate a 'repairability score' by examining the features of a specific product family. This process helps to identify the most appropriate evaluation criteria for that product range, such as key variables and target components, as well as determine the importance of each criterion. Other frequently used methods are the iFixit methodology, or labels like ONR 192102 (Austrian Standards, 2014), EN 45554 (The European Electrotechnical Committee for Standardization, 2024) and the French Indice de Réparabilité (FRI) (Ministère de la transition ecologique, 2024; M. de la Transition écologique). These semi-quantitative methods are usually combined with quantitative methods, such as the 'ease of Disassembly Method' (eDiM) (Vanegas et al., 2018), which uses the Maynard Operation Sequence Technique (MOST) to estimate the disassembly time for a component, taking into account the operator's skills and other relevant factors (Fazio et al., 2021).

Given that these methods often need tailoring to specific products, significant research has been conducted to adapt them to particular product categories. For instance, iFixit has devised a method specifically for evaluating the repairability of smartphones (Flipsen et al.), while the French Repairability Index (FRI) has applied similar approaches to vacuum cleaners, washing machines, dishwashers, TVs, laptops, smartphones, and lawnmowers (M. de la Transition écologique). However, no assessment method yet exists that is tailored specifically for the repairability of PV modules. This represents a significant research gap that must be addressed to enhance the circularity of PV module technology. Consequently, a comprehensive assessment framework for enhancing PV module repairability is designed and presented in the next section. It provides a tailored method able to compare the repairability level of different PV module designs or different modifications within one design.

2.2. Relative repairability assessment method for PV module designs

As most repairable PV modules are still in the concept phase, many quantitative methods prove too detailed for the concept stage, as specifics like the number of screws or disassembly steps are not yet determined. Additionally, quantitative methods often overlook many factors that contribute to 'repairability', as they only account for those that can be measured or calculated (Dangal et al., 2022). On the other hand, qualitative methods based on pass-fail criteria (Cordella et al., 2018) only allow to differentiate between 'good' and 'bad' products but not to assess the relative repairability of specific models. Therefore, for the assessment of PV module concepts, the qualitative method proposed by Cordella et al. (2018) is adapted to a semi-quantitative method to allow better differentiation between design options while preventing the need of detailed product information as needed in most quantitative methods. This method thus assesses the relative impact of different design changes, rather than relying on a single overall score. It focuses on evaluating how different design options or modifications within a design would affect repairability in relative terms. This is especially useful for *optimizing a design on repairability*, as it allows designers to make informed trade-offs and prioritize which modifications are most effective for improving repairability.

In Table 1, a list of criteria that influence the repairability of PV modules is presented. This list is based on the generic and non-exhaustive list of criteria for assessing the repairability and upgradability of products developed by Cordella et al. (2019) and is adapted to specifically address PV modules. A key modification includes integrating 'automation' into the Accessibility, Visibility, and Tools criteria, recognizing that PV modules are typically assembled and disassembled by machines. The criterion 'data deletion' has been excluded as it is irrelevant to PV modules. The definition of Technical Skills has been revised to reflect a more realistic scenario where the optimal situation is that the repair can be performed by any technician, rather than by the end-user. This adjustment acknowledges that PV modules are complex systems, and it is more realistic to expect professional technicians, rather than users, to handle repairs effectively in the case of PV modules. The final modification involves incorporating time into the definition of Disassembly and Reassembly. This change acknowledges that while a process may be achievable within a limited number of steps, it is equally important that these steps can be completed within a reasonable time frame. By including time, the definition better reflects the practical considerations of repair efficiency.

Table 2 outlines a relative scoring method based on these criteria. Each criterion is weighted (either 1, 2 or 3) according to its relative importance on repairability. A weight of 1 is assigned if the panel can still be repaired when this criterion is met, though it may require slightly more effort or time. For example, the 'Availability of maintenance and repair information' is assigned a weight of 1, as the lack of this information may make it more challenging for a technician to figure out how to repair the panel, though the repair can still be done. A weight of 2 is given when the absence of this criterion significantly complicates the repair, requiring considerable workarounds. A weight of 3 indicates that repair is practically impossible if this criterion is not met. For example, a weight of 3 is given to 'Disassembly and reassembly of parts' and 'Removability of fasteners and disassembly reversibility' as it is often impossible to repair parts when they cannot be disassembled, removed or reassembled. The weighting factor can be adapted to the application or the aim of the specific design and is therefore a slightly subjective decision for the engineer. However, the weighting is valuable since some criteria are interrelated. For instance, redesigning a concept to simplify the automation of the repair process (which is beneficial) might require more advanced tools (which is less favorable). The weighting factor can therefore help determine whether the overall impact on repairability is positive or negative. The scoring ranges from negative (−1) if the design change has a negative effect of this specific criterion, neutral (0) if no effect, to positive (1) if it positively affects this criterion.

Table 1
Repairability assessment criteria with definition.

Criterion	Definition
Identification of the problem	Causes of all key failures can be established easily because of available evidence (e.g. error codes provided directly by the product or in the user manual).
Availability of maintenance and repair information	Maintenance and repair information is provided by the manufacturer (printed or online).
Technical skills	Repair of key failures can be performed by any technician.
Availability of spare parts	Original and compatible spare parts are widely available for replacement.
Identification of parts	Parts are clearly distinguishable, engraved, marked, or labeled for quick identification and/or replacement.
Disassembly and reassembly of parts	All parts can be disassembled and reassembled in a limited number of steps and within a limited time span.
Accessibility of parts	All parts are readily accessible (i.e. attainable without requiring prior removal of other components) using tools or machines.
Visibility of fasteners	Fasteners used to assemble parts are visible to the human eye or to automated systems.
Removability of fasteners and disassembly reversibility	All connections are reversible and reusable.
Repair location limitations	Repair of parts can be performed on-site.
Degree of automation	The repair process can be fully automated.
Types of machinery and tools needed	Only basic machines or tools are required to disassemble parts.
State after repair/upgrade action	The product functions with no or minimal loss in quality (efficiency, power output) and aesthetics.
Updatability	The product is adaptable to market standards, allowing replacement of parts with newer versions available on the market.

Most methods found in literature typically focus on priority parts rather than all components (Formentini et al., 2025). These priority parts are generally identified based on criteria such as failure rates, technical or market considerations, or environmental and economic impacts. While this can be useful in later stages of development, the approach proposed in this work does not distinguish between priority and non-priority parts. This is because the method is primarily intended for use in the early design phase, where it is often still unclear which components will ultimately be considered priority parts. At this stage, the dimensions and characteristics of components can vary significantly. For instance, the glass layer could still be doubled in thickness. Thin glass is prone to breakage and would likely be classified as a priority part due to its high failure rate, whereas thicker glass may be significantly more robust and thus not prioritized. Also the environmental impact of a part is hard to estimate in this stage, as this depends heavily on the amount of material used. These quantities are still flexible during early design, which makes it difficult to make accurate assessments about which parts will have the most significant

Table 2
Method to assess relative repairability between different designs or design variables. Scores indicate the effect of an increase in the design variable.

Parameter (Weight)	−1	0 No impact	1
Identification of the problem (**2**)	Limits identification of failure causes via error codes or manuals	–	Improves identification of failure causes via error codes or manuals
Availability of maintenance and repair information (**1**)	Reduces availability of maintenance and repair information	–	Increases availability of maintenance and repair information
Technical skills (**1**)	Increases reliance on specialized technicians or companies	–	Reduces need for specialized repair skills
Availability of spare parts (**2**)	Reduces availability of original and compatible spare parts	–	Improves availability of original and compatible spare parts
Identification of parts (**1**)	Parts become less distinguishable	–	Parts become more distinguishable
Disassembly and reassembly of parts (**3**)	Increases number of steps or time required	–	Reduces number of steps or time required
Accessibility of parts (**2**)	Reduces accessibility for tools or machines	–	Improves accessibility for tools or machines
Visibility of fasteners (**2**)	Reduces fastener visibility	–	Improves fastener visibility
Removability of fasteners and disassembly reversibility (**3**)	Reduces reversibility or reusability of connections	–	Improves reversibility or reusability of connections
Repair location limitations (**1**)	Limits feasibility of on-site repair	–	Facilitates on-site repair
Degree of automation (**2**)	Reduces potential for repair automation	–	Improves potential for repair automation
Types of machinery or tools needed (**2**)	Requires more advanced or specialized tools	–	Enables use of basic, widely available tools
State after repair or upgrade (**2**)	Negatively affects quality or aesthetics	–	Improves quality or aesthetics
Updatability (**2**)	Limits replacement with newer component versions	–	Facilitates upgrading to newer component versions

environmental or economic impact. For that reason, the current method takes all parts into consideration equally, making it more suitable for early-stage assessments and optimization purposes where design variables have not yet been fixed.

2.3. Experiments

Experiments were performed using a vacuum-based suction setup shown in Fig. 3. These experiments were designed to closely follow the procedures outlined in the IEC61215 standard for mechanical load testing of PV modules. The mechanical load was applied, which exerted pressure on the front glass surface of the PV module. Deflection was measured 10 s after load application using a laser displacement sensor.

2.4. Simulation model development

To redesign and optimize the solar panel for repairability, a parametrized 3D model of the PV module was built in Solidworks. Next, a Livelink was created to connect the Solidworks model to COMSOL Multiphysics which was used to perform the finite element analysis (FEA). The material properties used in the model for different components in a solar panel are summarized in Table 3. FEA was performed by applying a uniform pressure of 2400 Pa to the front glass of the PV module, while fixed boundary conditions were applied at the mounting clamp locations. To reduce computational complexity, the ribbons and electrical wiring were not included in the model. The solar cells were modeled with dimensions of 182 mm × 91 mm ×0.50 mm, while both the adhesive dots and the edge seal were assigned a thickness of 1 mm.

Table 3
Material properties used in the model (Li et al., 2020; Lee and Tay, 2013).

Property	Al 6083-T6	Solar glass	PIB	Si
Density (kg/m^3)	2700	2500	1000	2329
Young's modulus (GPa)	69	74.8	0.01	185
Poisson ratio (–)	0.33	0.216	0.48	0.22
Yield strength (MPa)	215	42[a]	2.4	200
Tensile strength (MPa)	240	90–170	9	200[b]

[a] Design yield strength.
[b] Bending strength.

To decrease the computational time, only a quarter of the panel was modeled exploiting the symmetry of the design. Adhesive dots were modeled as bonded pairs. The mesh size was progressively reduced until the model's deformation results showed convergence to balance computational efficiency with adequate simulation accuracy. The 3D model was validated by comparing its predicted deflections with those measured in experiments under equivalent loading conditions. This model is then used for optimization under uncertain loading scenarios as explained in the next section.

2.5. Reliability-based optimization

Given that this study focuses on a concept-phase design, significant uncertainty exists due to the lack of precise data and extensive experimental validation. In early-stage development it is therefore useful

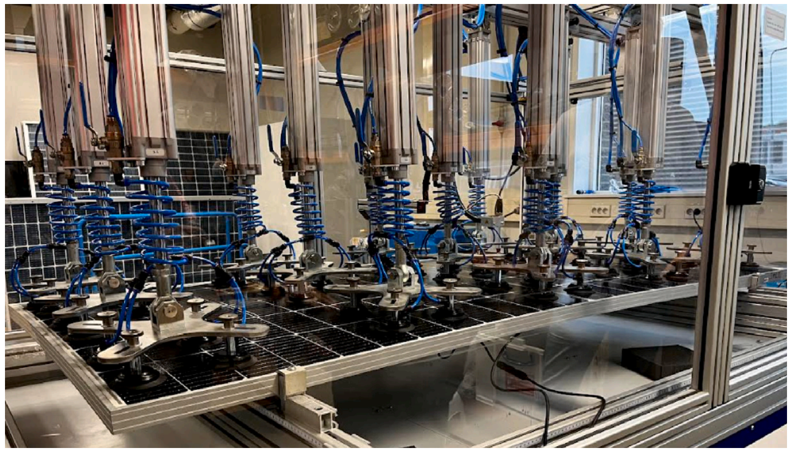

Fig. 3. Modular experimental setup capable of testing in various configurations.

to adopt an optimization approach that can systematically account for these uncertainties. In engineering design, Reliability-Based Design Optimization (RBDO) is used to optimize system performance while accounting for uncertainty in for example loads, material properties, or manufacturing tolerances (Chiralaksanakul and Mahadevan, 2004). These approaches are typically categorized based on how they integrate reliability analysis into the optimization loop. Double-loop methods, such as the Reliability Index Approach (RIA) and Performance Measure Approach (PMA), perform nested loops of optimization and reliability evaluation, but are often computationally expensive (Choi et al., 2007). Furthermore, surrogate-assisted methods reduce computational cost by using response surface models, such as Kriging or polynomial regression, to approximate expensive simulations (Choi et al., 2007). While these approaches offer significant potential, their application remains largely confined to specialized research domains (Nejadseyfi, 2025b). This limited adoption is partly due to the complexity and inaccessibility of existing tools. Their implementation can be complex and often requires custom programming or extensive tuning. Moreover, constructing surrogate models and the use of approximation methods such as Monte Carlo simulations for uncertainty quantification often impose substantial computational time. To address the limitations in existing optimization workflows, Nejadseyfi developed Robustimizer, an open-source educational and research software (Nejadseyfi, 2025a) with graphical user interface designed for efficient uncertainty quantification, robust optimization, and reliability-based optimization (RBDO) (Nejadseyfi, 2025b). By combining surrogate modeling with analytic formulations, the software enables fast and accurate exploration of uncertain design spaces with nonlinear objectives without the need for extensive custom coding. At the same time, it facilitates intuitive constraint handling through its graphical user interface. This program is particularly well suited for this case study, due to its demonstrated value in optimization processes aimed at reducing environmental impact particularly in contexts where effectively managing uncertainties is crucial. The next sections provide a detailed breakdown of the optimization framework used to optimize the Biosphere Solar PV Module.

2.5.1. Design variables

Table 4 provides an overview of the design variables with their bounds included in modeling and optimization. Additionally, Fig. 4 provides an overview of how the design variables are defined in the model. These variables represent all the adjustable elements within the existing design that influence stress and deformation in the panel without requiring an entirely new design concept.

2.5.2. Objective function

The aim of this optimization is to minimize a combined objective consisting of contributions from weight, cost, and repairability index while meeting the required mechanical performance.

$$\min_{\mathbf{x}} F_{\text{obj}}(\mathbf{x}) = \delta m(\mathbf{x}) - \delta r(\mathbf{x}) + \delta c(\mathbf{x}) \tag{1}$$

Where F_{obj} is the objective function [unitless, ratio], δm is the relative change in mass from the initial design [-], δr is the relative change of the Repairability [-] and δc is the relative change in total costs [-]. The objective function is minimized and therefore the negative sign for δr is required meaning that an increase in repairability is desired while mass and costs must be reduced. Since mass, repairability, and costs are considered equally important in this study, they are combined in the objective function without applying additional weighting factors. The use of equal weighting factors reflects the exploratory nature of this study. Applying equal weights avoids introducing subjective bias and allows the influence of mass, cost, and repairability to be assessed on an equal basis. In practical product development, these weighting factors may be adjusted to reflect manufacturer priorities, regulatory requirements, or business objectives. The proposed framework can be readily generalized to accommodate alternative weighting strategies.

The relative change in mass is defined by:

$$\delta m(\mathbf{x}) = \frac{m(\mathbf{x}) - m_0}{m_0} \tag{2}$$

Where m_0 is the mass of the original Biosphere module V1.3, and $m(\mathbf{x})$ is the total mass which depends on design variables. Both m_0 and $m(\mathbf{x})$ are a sum of the masses of all parts within the module including frame, sealant, cells, and electronics.

As discussed in Section 2.1 assigning an exact quantitative value to repairability is challenging. Nevertheless, it is often feasible to assess relative changes in repairability, namely whether a given design variable is expected to have a positive or negative influence on these factors. The contribution of the relative change in repairability (δr) to the objective is given by:

$$\delta r(\mathbf{x}) = \sum_i (RS_i \cdot \delta p_i) \tag{3}$$

where the Repairability Score (RS) for each variable is calculated with the Relative Repairability Method presented in Section 2.2 and δp_i is the relative change in parameter i.

2.5.3. Costs

To capture cost variations due to design changes, the relative cost is expressed as:

$$\delta c(\mathbf{x}) = \frac{c(\mathbf{x}) - c_0}{c_0} \tag{4}$$

Table 4
Design variable overview.

Variable	Initial value	Lower bound	Upper bound
h_f, Frame height (mm)	30	10	100
w, Clamping width (mm)	50	35	100
d_m, Mounting position (mm)	100	0	464
h_{g1}, Top glass thickness (mm)	2	2	4
h_{g2}, Bottom glass thickness (mm)	2	2	6
d_x, Horizontal distance between dots (mm)	140	20	396
d_y, Vertical distance between dots (mm)	100	20	188

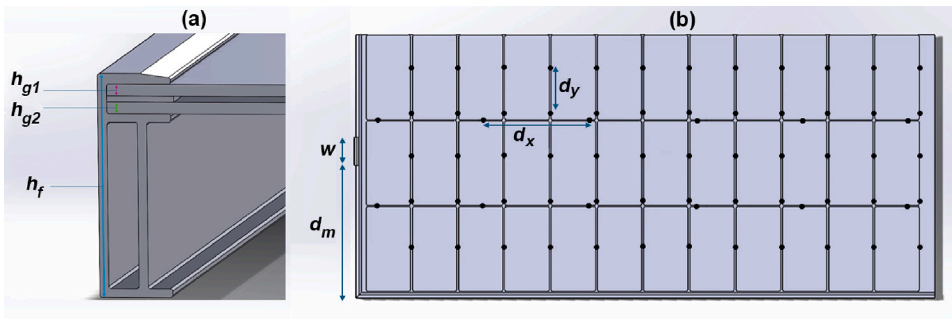

Fig. 4. Design variables for optimization.

The term c_0 is the cost for the reference design. The term $c(\mathbf{x})$ is the cost of the parametrized module and depends on the variables listed in Table 4. The total costs are the sum of the material costs, shipping costs, and production costs. The reference costs are the sum of the original material costs, shipping costs, and production costs of the Biosphere module V1.3.

$$c(\mathbf{x}) = c_{\mathrm{mat}}(\mathbf{x}) + c_{\mathrm{ship}}(\mathbf{x}) + c_{\mathrm{prod}}(\mathbf{x}) \tag{5}$$

2.5.4. Constraints

The constraints of the optimization problem are based on the IEC61215 standard for PV modules (International Electrotechnical Commission, 2021). According to this standard, a PV module must be able to withstand a static uniform pressure of 2400 Pascal on the front glass without causing visual damage to the panel. To meet these requirements, several constraints are imposed on the model. First, the maximum first principal stress in the front glass due to the uniform pressure of 2400 Pa, denoted by $\mathrm{sp1_g}$, must remain below the tensile strength of the glass. Due to uncertainties in the applied load, the calculated stress in the glass exhibits a statistical distribution rather than a single deterministic value. To ensure a conservative yet realistic safety margin, the stress constraint is formulated using a reliability based constraint. This approach aims at 99.7% confidence level under the assumption of a normal distribution. The resulting expression ensures that, with high probability, the maximum stress in the glass remains below its material tensile strength:

$$\mu_{\mathrm{sp1_g}}(\mathbf{x}) + 3\sigma_{\mathrm{sp1_g}}(\mathbf{x}) < \sigma_{\mathrm{g}}^{\mathrm{t}} \tag{6}$$

As mentioned in Table 3, $\sigma_{\mathrm{g}}^{\mathrm{t}}$ is set to 0.17 GPa during optimization. Similarly, the first principal stress in the silicon solar cells due to this pressure, $\mathrm{sp1_c}$, must stay below the tensile strength of silicon, $\sigma_{\mathrm{s}}^{\mathrm{t}} = 0.2$ GPa:

$$\mu_{\mathrm{sp1_c}}(\mathbf{x}) + 3\sigma_{\mathrm{sp1_c}}(\mathbf{x}) < \sigma_{\mathrm{s}}^{\mathrm{t}} \tag{7}$$

Finally, the maximum deflection of the glass, (δ_{g}), must not exceed a certain limit to prevent contact with the underlying mounting structure. For the Biosphere PV module design V1.3, the module is mounted on installation beams with a height of 50 mm and incorporates a frame height of 30 mm. Consequently, deflections exceeding $d = 0.08m$ would cause the glass to come into contact with the mounting structure, potentially resulting in glass fracture.

$$\mu_{\delta_{\mathrm{g}}}(\mathbf{x}) + 3\sigma_{\delta_{\mathrm{g}}}(\mathbf{x}) < d \tag{8}$$

Only the stresses in the glass and solar cells are evaluated, as in earlier tests these were identified as the most critical components in the design. The material properties used, including tensile strengths, are listed in Table 3. Note that for the scope of this paper, only the static forces are taken into account.

2.5.5. Uncertainties

Several factors contribute to uncertainty in the optimization problem, particularly regarding the uniform pressure applied to the top glass of the PV module. First, real-world conditions and testing setups can introduce slight variations in the way pressure is applied, such as uneven loading or equipment inaccuracies causing the actual load to deviate from the intended value. Second, 3D modeling inherently approximates reality. Geometric simplifications and numerical limitations (e.g., finite mesh size) introduce modeling errors. Third, material and manufacturing inconsistencies such as variations in surface texture, flatness, or internal structure can lead to different stress distributions under identical loading conditions (Barry, 2010).

Therefore, when analyzing or simulating the behavior of a solar module under load, it is both realistic and more robust to account for uncertainties in the applied load. Instead of assuming a fixed pressure, the pressure applied to the model is therefore expressed as:

$$p = 2400[\mathrm{Pa}] * \xi \tag{9}$$

Here, ξ represents the uncertainty on the load, which can follow various distributions (e.g., normal, uniform, log-normal). To estimate the uncertainty distribution, real-life prototype testing was conducted to gain insight into the variability in output responses. The observed deflection data from these tests was then used to approximate the corresponding input variation by comparing it with simulated outputs using different candidate distributions for ξ. This comparison was performed using COMSOL's *Uncertainty Quantification* module. By tuning the input distribution of ξ, a match was found between the simulated output and the real-life measurements. A normal distributed ξ with mean $\mu_\xi = 1.03$ and standard deviation $\sigma_\xi = 0.013$ yielded a predicted deflection distribution with a mean $\mu_{def} = 34.0$ mm and standard deviation $\sigma_{def} = 0.41$ mm which closely matches the experimental results.

3. Results and discussion

3.1. Repairability based on design modifications

The Relative Repairability Method, described in Section 2.2, is applied to each of these potential design modifications to assess their impact on the overall repairability of the design. A thicker glass sheet will likely result in a more repairable design (RS 5/26). This is mainly due to the fact that a thicker glass will less easily break making it easier to carry or transport. A thicker frame, at least within reasonable thicknesses, has limited impact on the overall repairability (RS 0/26). Also the size and the location of the mounting clamps seem to have no noticeable impact (both RS 0/26). Increasing the amount of adhesive dots will result in a significantly lower repairability of the design (RS -8/26). This indicates that from a repairability point of view alone, the most effective approach would be to increase the glass thickness and, if necessary, adjust the frame thickness and mounting clamp design to ensure the panel can withstand a minimum load of 2400 Pa. However, maximizing repairability must be balanced with cost and mass constraints to ensure a practically viable design. Because the trade-offs between these factors are complex and not easily optimized through manual iteration, optimization techniques are applied to systematically identify the best design configuration.

3.2. Experimental and numerical results

To validate the results of the FEA conducted using the COMSOL model, physical experiments were performed using a vacuum-based suction setup shown in Fig. 3. These experiments were designed to closely follow the procedures outlined in the IEC61215 standard for mechanical load testing of PV modules. However, as the application of a full 2400 Pa static load caused immediate failure of the initial module, the applied load was reduced to 1000 Pa to prevent damage and allow for meaningful comparison between the simulations and experiments. Deflection was measured 10 s after load application using a laser displacement sensor positioned at a defined location: 175 mm from the center of the panel (see red dot in Fig. 5). To ensure consistency between the experimental and numerical results, the COMSOL model was configured to replicate the loading conditions used in the experiment, including the exact positions of the suction cups. The simulation results were then evaluated at the same probe point as in the experimental setup. The test was repeated 18 times on each of two PV modules with identical designs, in order to assess the variability both within and between the samples.

The simulated deflection is shown in Fig. 5. The maximum simulated deflection was 33.7 mm at the center, and 33.2 mm at the measurement location used in the experimental setup, while the experimental setup provided a mean value of 34.0 mm with a standard deviation of 0.41 mm. This corresponds to an average deviation of 2.4%, indicating good agreement between simulations and experiments.

In addition to deflection, the simulation also assessed tensile stress in the solar cells (see Fig. 6). Several regions, particularly near the long edges, showed stress levels exceeding the tensile strength of crystalline silicon (0.2 GPa), indicating the risk of microcrack formation. To confirm this prediction, Electroluminescence (EL) imaging was conducted before and after testing. Fig. 6 shows the results, where dark spots on the post-test image confirm the presence of electrical defects, such as microcracks formed during loading. However, it must be noted that the largest observed crack did not align exactly with the location of highest simulated stress. One possible reason for this discrepancy is the simplifications made in the model (for example, the omission of wires and electronics); see also Section 4.

With the validated model, the effects of different design choices and various configurations can be investigated. Fig. 7(a), shows that increasing the frame height has a substantial impact on cost, while its effect on mass is minor and its influence on repairability is negligible. The increase in cost is primarily driven by higher shipping costs rather than material consumption. Conversely, Fig. 7(b) demonstrates that frame thickness significantly affects the stresses in the solar cells and the overall panel deformation. Importantly, the marginal benefit of increasing frame thickness is greatest at lower thicknesses; as the frame becomes thicker, additional increases yield progressively smaller reductions in stress and deformation. From Fig. 7(c) on the other hand, it can be observed that increasing the glass thickness has a positive effect on the repairability of the module but also a high effect on the mass of the entire PV module. It has no effect on the costs of the module, as the price change for glass is negligible for different glass thicknesses within the defined range. Fig. 7(d) indicates that the glass thickness affects the stresses in the solar cells and glass, and a slightly lower but visible effect on the overall panel deformation. As expected, increasing either variable reduces cell stress. However, an important observation is that frame thickness has a considerably stronger effect on stress reduction than glass thickness. The current model suggests that, for minimizing cell stress, prioritizing an increase in frame thickness is much more effective than increasing the glass thickness. Overall, to increase structural strength, using a thicker frame is more efficient in terms of weight, whereas thicker glass is generally more economical and benefits repairability.

3.3. Optimization

To determine the optimal design configuration of the Biosphere PV module, the optimization framework described in Section 2 was applied. The initial optimization run was performed using a design of experiments (DOE) consisting of 70 points. Subsequently, three additional infill points were incorporated iteratively to refine the DOE until the solution stabilized. Based on the output from the simulations, a surrogate model was constructed. Leave-One-Out Cross-Validation (LOOCV) results indicate that the surrogate model for the main response (objective function) has good predictive performance, indicating a reliable surrogate model (see 8(a)). This was expected due to the linearity in the objective function. Additionally, the surrogate models for the deformation constraint 8(b), the stress in the glass (Fig. 8(c)) and the stress in the solar cell (Fig. 8(d)) exhibit sufficient accuracy.

3.4. Optimum design variables

Table 5 summarizes the optimized variable values for the Biosphere PV module design.

Several notable observations can be made regarding the resulting optimal configuration. Firstly, the optimized frame height is almost unchanged (only 9.3% decrease, see also Table 5). Not only does increasing frame thickness have a significant influence on the structural strength of the module but also significantly increases the shipping costs of the module. Secondly, the optimization resulted in a minimal number of adhesive dots (20 in total, a decrease of 94%), with a strong preference for larger dot sizes. Since both small and large adhesive dots contribute equally to the repairability score, the optimizer favors larger dots due to their superior mechanical performance in stress mitigation. The glass thickness is also increased compared to the original design, aligning with expectations. Thicker glass not only enhances structural performance and reduces deformation but also improves repairability by reducing fragility. However, the optimizer avoids excessively thick glass, balancing these benefits against the associated weight penalty. The clamp width is increased (27.8%) and moved to the corner of the PV module so as to optimally reduce the stress around the mounting clamp.

These variables altogether achieve an objective function value of −0.0928 while satisfying the imposed constraints on deformation and allowable stresses within both the solar cells and glass layers, see also Fig. 9.

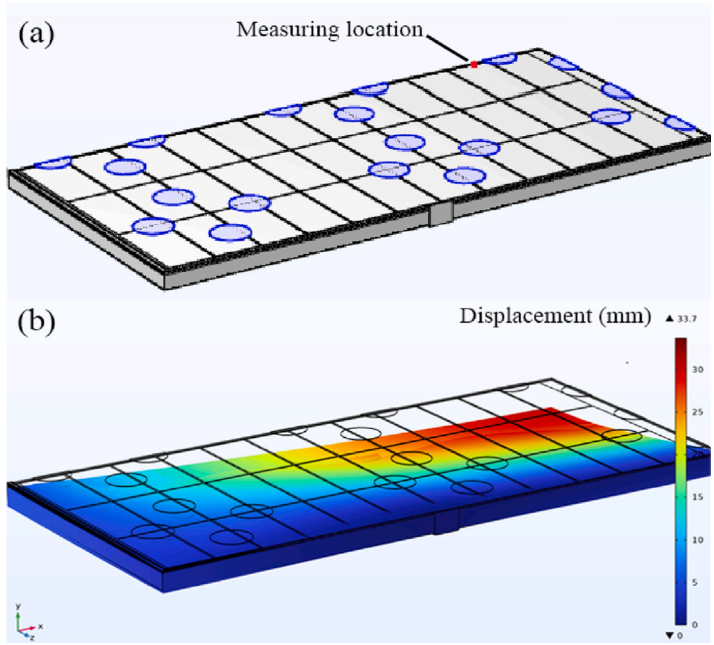

Fig. 5. (a) COMSOL model showing pressure locations and measurement point. Due to symmetry, only one-quarter of the module is simulated, (b) Simulated deflection of the quarter model under 1000 Pa loading.

Table 5
Optimized design variable values for the Biosphere PV module and their relative change compared to version V1.3.

Variable	h_f	w	d_m	h_{g1}	h_{g2}	d_x	d_y
Optimum (mm)	27.2	63.9	0.0	3.4	2.8	396.0	177.1
Relative change	−9.3%	+27.8%	−100%	+70%	+40%	+183%	+77%

Table 6
Comparison of key characteristics for a traditional laminated PV module, the current Biosphere V1.3 design, and the optimized Biosphere V1.3 module.

Variable	Traditional PV module	Biosphere V1.3	Optimized Biosphere V1.3
Structural static strength	Passes IEC 61215	Fails IEC 61215	Passes IEC 61215
Repairability	Nearly impossible	Possible in some cases	Achievable in most cases (+51% vs. V1.3)
Mass	37.9 kg/module	32.5 kg/module	47.2 kg/module (+45% vs. V1.3)
Cost	Not comparable	—	6% lower vs. V1.3

Although the optimization aims to minimize the objective function, the optimal value is close to zero. In theory, a significantly negative Fobj would indicate an overall good improvement in mass, repairability, and cost relative to the reference design. However, such a result is practically unrealistic as the original design fundamentally lacks the mechanical strength to meet the required strength conditions. A design yielding a large negative Fobj would likely be structurally insufficient. Therefore, this slightly negative Fobj reflects the necessary trade-off: the module must be reinforced to endure a static load of 2400 Pa, resulting in moderate increases in weight and cost, with some impact on repairability, compared to the reference design.

Table 6 presents a comparative overview of the key characteristics of a conventional laminated PV module, the Biosphere V1.3 design, and the optimized V1.3 module. The optimized module demonstrates a substantial improvement in repairability, primarily due to the reduction in adhesive dots and the increase in glass thickness. These changes result in fewer irreversible and difficult-to-disassemble connections, as well as more robust and accessible components. Furthermore, the optimized design incurs marginally lower costs than the original V1.3 version, owing to reduced consumption of PIB for adhesive dots and aluminum for the frame, along with slightly lower shipping costs due to a more compact frame configuration. It should be noted that the cost

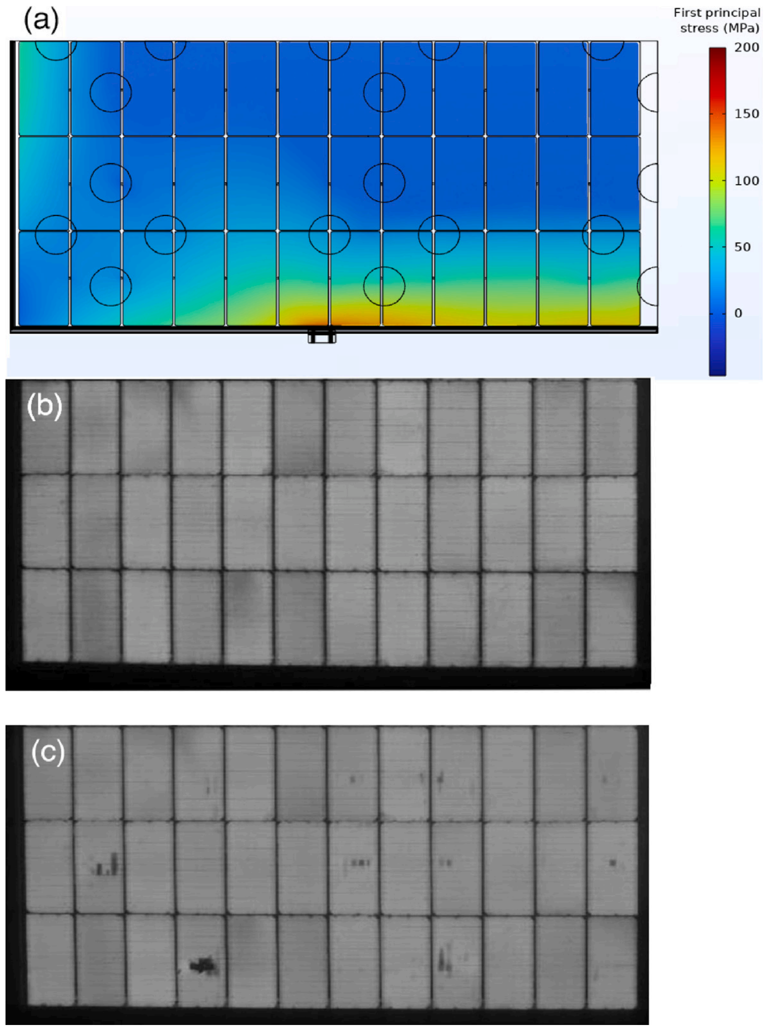

Fig. 6. Comparison of (a) principal stresses in solar cells of quarter module due to uniform pressure of 1000 Pa and (b) Electroluminescence image of quarter module before loading and (c) Electroluminescence image after applying 1000 Pa. Dark spots indicate micro-crack formation.

comparison is restricted to the Biosphere V1.3 and optimized Biosphere V1.3 designs. The Biosphere module is currently produced in small quantities, with production and shipping costs estimated specifically for this design concept. As conventional laminated PV modules are manufactured at a vastly different production scale using highly optimized industrial processes, a direct comparison of absolute costs would not be meaningful and could lead to biased conclusions. Therefore, the costs of conventional PV modules are not reported in Table 6, and only relative cost differences between the Biosphere designs are considered. Nevertheless, the economic competitiveness of laminate-free PV architectures should not be assessed solely on the basis of current manufacturing costs. Conventional laminated PV modules benefit from decades of process optimization and large-scale production, whereas repairable PV concepts remain at an early stage of development. It is therefore plausible that a substantial portion of the current cost gap could be reduced through manufacturing scale-up and process optimization. Furthermore, if repairability leads to longer service lifetimes and reduced replacement rates, a higher initial manufacturing cost may still be economically justified from a life-cycle perspective. Finally, the optimized module exhibits significantly enhanced mechanical strength compared to the original Biosphere V1.3 design, however, this improvement comes at the cost of increased overall weight, with the module mass rising by approximately 45%. It should be noted that the optimization was performed for a fixed module architecture, area, and power output. However, future generations of repairable PV modules are not necessarily constrained to the same geometry or design concept. Alternative module layouts, materials, frame configurations, or dimensions may provide different trade-offs between repairability, structural reliability, and mass. Therefore, the observed mass increase should not be interpreted as a fundamental limitation of repairable PV architectures in general.

3.5. Uncertainty quantification at optimum design

To assess the reliability of the optimal design under the input uncertainty, a Monte Carlo simulation was performed using the surrogate model. Fig. 10 displays the outcome distributions for the three

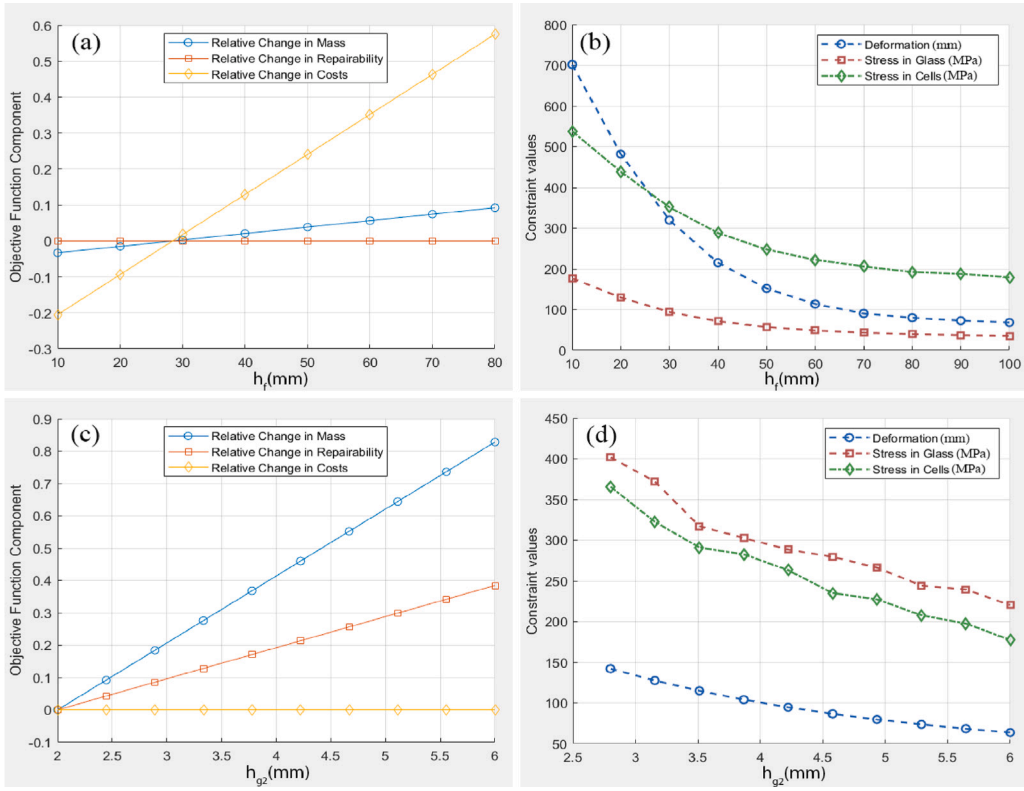

Fig. 7. Effect of glass thickness and frame height on the objective function and constraints.

constraint functions evaluated at the optimized design. Each histogram shows how certain responses vary due to uncertainty, with the horizontal axis representing the constraint response value and the vertical axis showing the frequency. As can be seen in Figs. 10(a), 10(b) and 10(c), all constraints are satisfied, while both stress constraints are active, the constraint on deformation remains much below the set value.

4. Limitations, recommendations, and future work

One significant limitation of the applied repairability assessment method is its inherent subjectivity. The weighting factors, which determine the relative importance of each criterion, are subjective and depend on the aim and judgment of the engineer conducting the assessment. This subjectivity can also extend to scoring criteria, such as what constitutes a 'clearly' visible fastener or an 'accessible' component. As a result, different evaluators might arrive at slightly different scores for the same design. Further research is required to refine and standardize the weighting factors, particularly to better understand which aspects of repairability are most critical and which may be less relevant. Such weighting factors could be established through expert consensus approaches (e.g., the Delphi method), industry-wide guidelines, analysis of historical repair and failure data, or a combination thereof. This would improve the reproducibility and comparability of repairability assessments across different engineering teams and organizations. Nevertheless, the inherent uncertainty associated with these assessments can be incorporated as input uncertainty during the design stage and explicitly accounted for through uncertainty quantification, robust optimization, or reliability-based design optimization. To gather the uncertainty in the repairability index, many experts can contribute to assigning these weights independently providing probabilistic input to the optimization algorithm.

Another methodological limitation lies in the assumption of linearity. The method presumes that the impact of a variable on repairability is linear: i.e., doubling the variable results in double the effect. In reality, these relationships are likely to be non-linear, which may lead to different outcomes in the optimization. Further research is recommended to accurately characterize the relationship between specific design variables and their impact on repairability.

The 3D model has several simplifications that introduce limitations. Certain components such as wiring, electronics, and cutouts in the glass have been omitted to reduce modeling complexity. Additionally, the frame geometry has been slightly simplified. Although validation has shown that these omissions do not significantly affect static stress results, their influence might be more critical in dynamic or thermal analyses. The validation of the model introduces its own uncertainties. The validation tests could only measure the deflections at a single location with limited accuracy (> 0.25 mm). Moreover, there might be some inaccuracies in the applied pressure due to equipment limitations.

Only two panels were tested, and deviations were observed not only between seemingly identical panels, but also between repeated measurements on the same panel. This suggests that manual assembly steps and manufacturing variability have a noticeable influence on the structural performance. Because the uncertainty distribution used in the numerical analysis was calibrated from the experimental measurements, the adopted uncertainty model captures the combined effect of several real-world uncertainty sources, including loading, material, manufacturing, and assembly-related variations. Future studies should include a larger number of prototypes and multiple measurement techniques to further improve the characterization and separation of these uncertainty sources.

The scope of this research was restricted to evaluating static loading conditions. However, for a comprehensive mechanical analysis of PV modules, dynamic and impact loading as well as thermal stresses

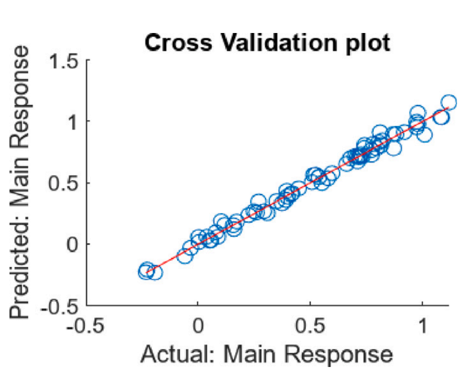

(a) LOOCV for the objective function (RMSE: 0.03885, R^2: 0.9879). Predictions closely match actual values

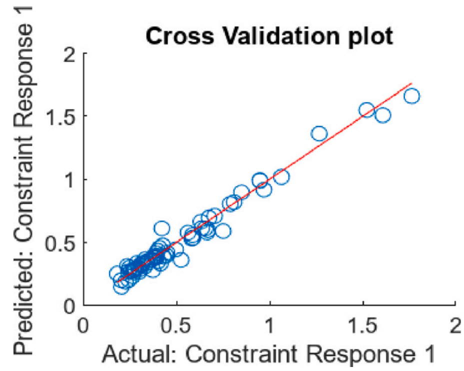

(b) LOOCV for the deformation constraint (RMSE: 0.05523, R^2: 0.9716). The model demonstrates good predictive performance.

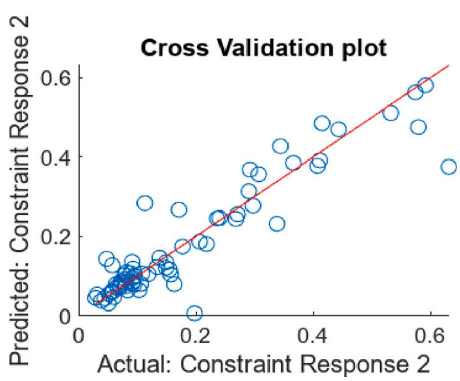

(c) LOOCV for stress in glass (RMSE: 0.05674, R^2: 0.8637). The model demonstrates sufficient predictive performance.

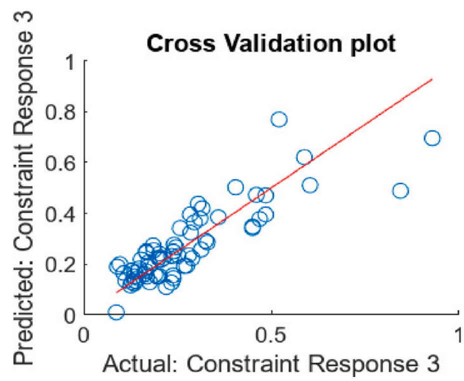

(d) LOOCV for stress in solar cells (RMSE: 0.08496, R^2: 0.7188). The model demonstrates sufficient predictive performance.

Fig. 8. Leave-One-Out Cross-Validation (LOOCV) performance of the surrogate models used in the optimization framework. Predictive performance is indicated by the Root Mean Square Error (RMSE), which should be close to zero, and the coefficient of determination (R^2, quantifying how well the predicted values correlate with the true values), which should be close to one. The objective function and deformation constraint models show high reliability, while the stress models for glass and solar cells show acceptable but slightly lower accuracy.

should be included. These additional effects could significantly alter the design trade-offs and optimization outcomes. For instance, the inclusion of thermal loading could alter the optimal configuration of the top and bottom glass thicknesses. While both glass layers exhibit similar thermal expansion behavior, differences in thickness modify the flexural rigidity of the module and influence the stress distribution under combined thermal and mechanical loading. Additionally, incorporating dynamic loads into the optimization framework could shift the optimal design toward configurations with a greater number of adhesive dots. Unlike the static load test, which applies only compressive forces, the dynamic load test specified in the IEC61215 standard subjects the module to alternating tensile and compressive forces (International Electrotechnical Commission, 2021). This bidirectional loading increases the mechanical demands on the adhesive bonds, potentially necessitating more or stronger adhesive connections to ensure structural integrity. Furthermore, while this study focused exclusively on repairability as a circularity metric, future research could expand the scope to include other key aspects such as recyclability, reuse, and remanufacturing potential for a more holistic approach. Many of the identified limitations stem from the limited availability of detailed information which is a consequence of the design still being in its early development stage. Manufacturers often treat technical specifications, material compositions, and production methods as proprietary information, resulting in limited publicly accessible data. This lack of transparency hinders independent evaluation and comparison of design choices, particularly with regard to circularity, reparability, and sustainability. Promoting more open data exchange in the solar industry would greatly benefit research, innovation, and responsible product development.

5. Conclusions

This study demonstrates how repairability can be systematically integrated into photovoltaic (PV) module design without compromising structural performance or economic feasibility. A semi-quantitative relative repairability assessment method tailored to PV modules was developed and embedded within a reliability-based optimization framework. This approach enables repairability to be treated as a measurable design variable rather than a qualitative afterthought, thereby addressing a key gap in the current literature.

Applied to a laminate-free Biosphere Solar PV module V1.3, the methodology illustrates how structural requirements, cost constraints, and repairability objectives can be balanced simultaneously. Although the resulting module exhibits an increase in mass, this reflects the

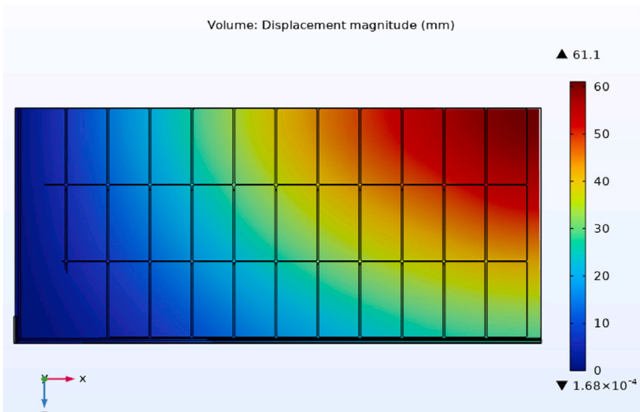

(a) Deformation distribution of the optimized design.

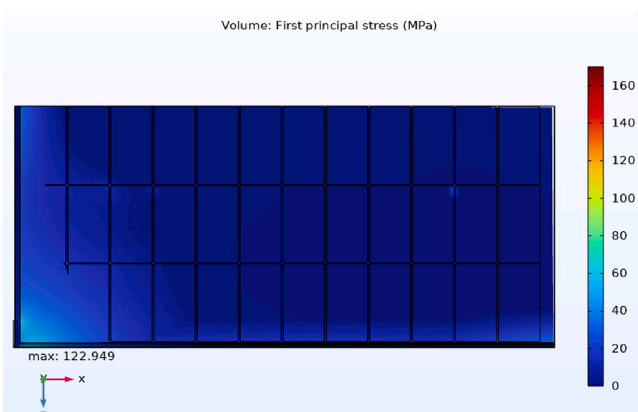

(b) Stress distribution in the solar glass for the optimized design.

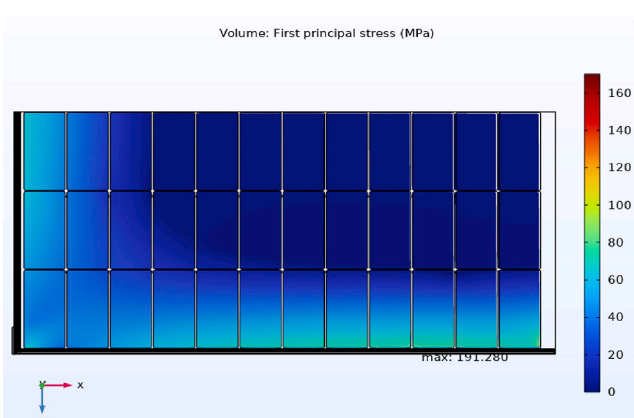

(c) Stress distribution in the solar cells for the optimized design.

Fig. 9. Simulation results of the optimized Biosphere PV module. Note that only a quarter of the module is displayed.

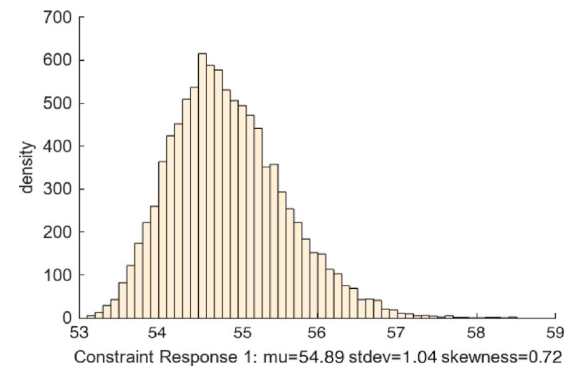

(a) Response distribution for the deformation constraint.

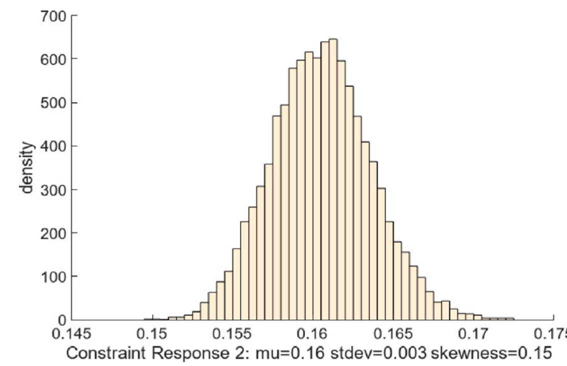

(b) Response distribution for the glass stress constraint.

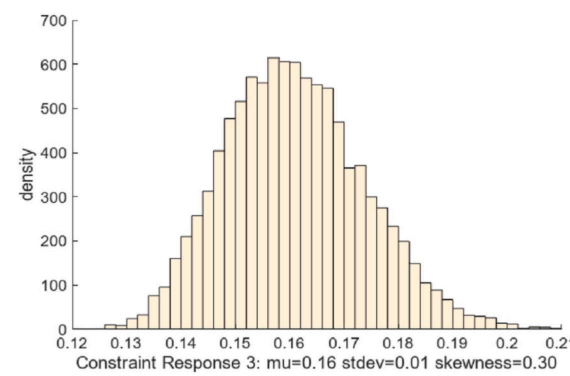

(c) Response distribution for stress in the solar cells

Fig. 10. Reliability constraints at the optimum design, quantifying the robustness of the solution under input uncertainty.

structural reinforcement necessary to meet mechanical standards rather than inefficiencies in the optimization process. The reliability-based formulation further reduces dependence on conservative safety margins by explicitly accounting for uncertainties in loading and subjective assessment criteria.

Application of the proposed framework to the Biosphere PV module resulted in a design that satisfies IEC61215 static load requirements while increasing the repairability score by 51% compared to the baseline design. The optimization further reduced costs by approximately 6% through material savings and design adjustments. Achieving the required structural performance, however, required an increase in module mass of approximately 45%, highlighting the inherent trade-off between repairability, weight, cost, and structural reliability in laminate-free PV modules.

Several limitations remain, including the subjectivity of weighting factors, the assumption of linear relationships in the repairability model, simplified finite element representations, and restriction to static loading conditions. Future work should refine the repairability metric, incorporate dynamic, impact resistance, and thermal effects, and expand the circularity scope to include recyclability and reuse potential.

This work demonstrates that repairability can be treated as a quantitative engineering design objective alongside structural reliability, enabling circular-design principles to be incorporated from the earliest stages of photovoltaic module development. Overall, the proposed framework provides a scalable foundation for integrating circular design principles into early-stage PV module development and supports more resilient and sustainable solar technologies.

CRediT authorship contribution statement

A.G. Timmers Verhoeven: Writing – original draft, Visualization, Validation, Software, Formal analysis, Data curation, Conceptualization. **Z. Fung-A-Jou:** Validation, Supervision, Resources, Methodology, Investigation, Formal analysis, Data curation, Conceptualization. **S. Brinksma:** Project administration, Methodology, Investigation, Funding acquisition, Conceptualization. **O. Nejadseyfi:** Writing – review & editing, Supervision, Software, Resources, Project administration, Methodology, Investigation, Conceptualization.

Declaration of competing interest

The authors declare that they have no conflicts of interest to report.

Acknowledgments

This publication is partially part of the project "Circular Multicolour BIPV factory" (STIM-00604) that is funded by the European Union as part of the OPZuid EFRO program for transition-driven innovation. The DML tests were carried out by the Netherlands Organisation for Applied Scientific Research (TNO) Solar Energy department as part of this subsidy. The authors would like to thank Biosphere B.V. for providing the open-source hardware design for this study.

Data availability

All data and codes are available at https://github.com/atimmersverhoe/RobustimizerSolar.

References

AL-Rousan, N., AL-Najjar, H., 2024. Optimized deep neural network to estimate orientation angles for solar photovoltaics intelligent systems. Clean. Eng. Technol. 20, 100754.
Austrian Standards, 2014. Onr 192102: 2014 - gütezeichen für langlebige, reparaturfreundlich konstruierte elektrische und elektronische geräte. URL: https://www.austrian-standards.at/de/shop/onr-192102-2014-10-01~p2091192.
Baldé, C., Kuehr, R., Yamamoto, T., McDonald, R., D'Angelo, E., Althaf, S., Bel, G., Deubzer, O., Fernandez-Cubillo, E., Forti, V., et al., 2024. Global e-waste monitor 2024.
Barry, C., 2010. Why Glass Sometimes Breaks. IEEE.
Blanco-Espeleta, E., Pérez-Belis, V., Bovea, M., 2024. Repair index of energy-related products: Application to capsule coffee machines. Sustain. Prod. Consum. 46, 146–160.
Bracquené, E., Brusselaers, J., Dams, Y., Peeters, J., Schepper, K., Duflou, J., Dewulf, W., 2018. Repairability criteria for energy related products study in the benelux context to evaluate the options to extend the product life time final report.
Chiralaksanakul, A., Mahadevan, S., 2004. Reliability-based design optimization methods. J. Mech. Des. 851–857.
Choi, S., Canfield, R., Grandhi, R., 2007. Reliability-based Structural Design. Springer London.
Chowdhury, P., Das, P., Chowdhury, H., Chowdhury, T., Bontempi, E., Corkish, R., 2026. Assessing tin demand and supply pressures under terawatt-scale photovoltaic deployment. Rsc Sustain. 4 (3), 1581–1592.
Chowdhury, T., Dehghanimadvar, M., Chang, N., Corkish, R., 2026. Evaluating short-circularity pathways for photovoltaic glass through life cycle assessment: Cullet recycling versus whole-glass reuse. Sol. Energy Mater. Sol. Cells 300, 114227.
Chowdhury, M., Rahman, K., Chowdhury, T., Nuthammachot, N., Techato, K., Akhtaruzzaman, M., Tiong, S., Sopian, K., Amin, N., 2020. An overview of solar photovoltaic panels' end-of-life material recycling. Energy Strat. Rev. 27, 100431.
Cordella, M., Alfieri, F., Forner, J., 2019. Analysis and development of a scoring system for repair and upgrade of products. EUR 29711 EN, no. KJ-NA-29711-EN-N.
Cordella, M., Sanfelix, J., Alfieri, F., 2018. Development of an approach for assessing the reparability and upgradability of energy-related products. Procedia CIRP 69, 888–892.
Dangal, S., Faludi, J., Balkenende, R., 2022. Design aspects in repairability scoring systems: Comparing their objectivity and completeness. Sustainability 14 (14).
Dupuis, J., Saint-Sernin, E., Nichiporuk, O., Lefillastre, P., Bussery, D., Einhaus, R., 2012. Nice module technology - from the concept to mass production: A 10 years review. In: Conference Record of the IEEE Photovoltaic Specialists Conference. pp. 003183–003186.
Einhaus, R., Madon, F., Degoulange, J., Wambach, K., Denafas, J., Lorenzo, F., Abalde, S., Delgado, T., Bollar, A., 2018. Recycling and reuse potential of nice pv-modules. pp. 561–564.
Fazio, F., Bakker, C., Flipsen, B., Balkenende, R., 2021. The disassembly map: A new method to enhance design for product repairability. J. Clean. Prod. 320, 128552.
Flipsen, B., M. depypere, M.H., Opsomer, T., Smartphone reparability scoring: Assessing the self-repair potential of mobile ict devices. PLATE 2019.
Formentini, G., Prioli, J., Ko, J., Hapuwatte, B., Ferrero, V., Badurdeen, F., Rickli, J., Ramanujan, D., 2025. A review of disassembly systems for circular product design. J. Clean. Prod. 506, 145459.
Foster, G., Kastanaki, E., Beauson, J., Neuwahl, R., and Marschinski, F., 2025. Circular economy strategies for the eu's renewable electricity supply. no. KJ-01-25-001-EN-N,.
Haegel, N., Verlinden, P., Victoria, M., Altermatt, P., Atwater, H., Barnes, T., Breyer, C., Case, C., Wolf, S.D., Deline, C., et al., 2023. Photovoltaics at multi-terawatt scale: Waiting is not an option. Science 380 (6640), 39–42.
International Electrotechnical Commission, 2021. International standard iec 61215-1: Terrestrial photovoltaic (pv) modules - design qualification and type approval.
Karagöz, S., Gündoğdu, T., Sarıaltın, H., Çeliktaş, M., 2025. A novel enzymatic delamination method for sustainable recycling of crystal silicon photovoltaic (c-si pv) modules. Sep. Purif. Technol. 361, 131373.
Khetri, M., Gupta, M., 2025. Recycling of silver from cigs solar cells using laser ablation and debonding. Sol. Energy Mater. Sol. Cells 282, 113381.
Kirchherr, J., Piscicelli, L., 2019. Towards an education for the circular economy (ece): Five teaching principles and a case study. Resour. Conserv. Recycl. 150, 104406.
Lee, Y., Tay, A., 2013. Stress analysis of silicon wafer-based photovoltaic modules under iec 61215 mechanical load test. Energy Procedia 33, 265–271, PV Asia Pacific Conference 2012.
Li, Y., Xie, L., Zhang, T., Wu, Y., Sun, Y., Ni, Z., Zhang, J., He, B., Zhao, P., 2020. Mechanical analysis of photovoltaic panels with various boundary condition. Renew. Energy 145, 242–260.
M. de la Transition écologique, Instructions manual for the display and the calculation of the repairability index of electrical and electronic equipments. Ministère de la Transit. Écologique 2022.
Majdi, A., Alqahtani, M., Almakytah, A., Saleem, M., 2021. Fundamental study related to the development of modular solar panel for improved durability and repairability. IET Renew. Power Gener. 15 (7), 1382–1396.
Ministère de la transition ecologique, 2024. Indice de réparabilité. URL: https://www.ecologie.gouv.fr/politiques-publiques/indice-reparabilite.
Ndalloka, Z., Nair, H., Alpert, S., Schmid, C., 2024. Solar photovoltaic recycling strategies. Sol. Energy 270, 112379.
Nejadseyfi, O., 2025a. Robustimizer. https://github.com/onejadseyfi/Robustimizer.
Nejadseyfi, O., 2025b. Robustimizer: A graphical user interface application for efficient uncertainty quantification, robust optimization, and reliability-based optimization of processes and designs. SoftwareX 30, 102077.
Padhamnath, P., Nalluri, S., Kuśmierczyk, F., Kopyściański, M., Karbowniczek, J., Kozieł, T., Leow, S., Reindl, T., 2025. Development of pv panel recycling process enabling complete recyclability of end-of-life silicon photovoltaic panels. Sol. Energy Mater. Sol. Cells 286, 113571.
Rodríguez, N., Favi, C., 2022. Eco-design guidelines takeaways from the analysis of product repairability and ease of disassembly: a case study for electric ovens. Procedia CIRP 105, 595–600.
Sivagami, K., Bose, S., Vinayak, A., Sreenivas, M., Ghosh, A., Narasimhan, M., Gurumoorthy, A., 2024. Solar panel recycling from circular economy viewpoint: A review. Appl. Sol. Energy 60, 328–345.
Späth, M., Wieclawska, S., Sommeling, P., Lenzmann, F., Balancing costs and revenues for recycling end-of-life pv panels in the netherlands. TNO report 2022 R10860, p. 2022.
Spiliotopoulos, C., Alfieri, F., Placa, M., E. Bracquené, E.L., Moeseke, T., Duflou, J., Dangal, S., Arriola, J., Flipsen, B., Faludi, J., Balkenende, R., Product reparability scoring system: Specific application to smartphones and slate tablets. Publ. Off. Eur. Union 2022.
Srithar, K., Udhayakumar, P., Sundhar, M., Baskar, P.G., Hemakumar, R., Saravanan, R., 2025. Photovoltaic panel with bottom-mounted air cooling system. Clean. Eng. Technol. 24, 100870.
The European Electrotechnical Committee for Standardization, 2024. European standardization. URL: https://www.cencenelec.eu/.
Vanegas, P., Peeters, J., Cattrysse, D., Tecchio, P., Ardente, F., Mathieux, F., Dewulf, W., Duflou, J., 2018. Ease of disassembly of products to support circular economy strategies. Resour. Conserv. Recycl. 135, 323–334.
Wambach, K., 2009. Photovoltaics recycling scoping workshop. In: 34th PV Specialists Conference, Philadelphia.
Weckend, S., Wade, A., Heath, G., End-of-life management: Solar photovoltaic panels. IEA-PVPS IRENA 2016.
Yao, Z., Tong, J., Gonçalves, R., Kumar, A., Manić, N., Vegliò, F., Romano, P., Jiang, J., Cui, J., Liu, J., Qi, W., 2025. Recycling of end-of-life solar panels: Focusing on the pyrolysis conversion of back sheet from a micro perspective. J. Clean. Prod. 490, 144796.